Check for updates

Iron-based nanozymes induced ferroptosis for tumor therapy

Chi Deng,†[a] Zichen Ye,†[a] Chunyue Joey Zheng,[b] Hongfei Cheng [ID] *[c] and Jingjie Ge [ID] *[a]

Iron-based nanozymes are an emerging class of nanomaterials demonstrating significant potential in tumor therapy by inducing ferroptosis—a regulated form of cell death marked by iron-mediated lipid peroxidation (LPO). These nanozymes exhibit unique enzymatic activities, including peroxidase, oxidase, and glutathione oxidase-like functions, enabling them to generate reactive oxygen species (ROS) and disrupt tumor microenvironment homeostasis. Leveraging Fenton chemistry, iron-based nanozymes amplify oxidative stress within tumor cells, thereby overcoming therapeutic challenges such as drug resistance and nonspecific toxicity. Despite significant advancements, the precise mechanisms by which iron-based nanozymes influence ferroptosis and their therapeutic efficacy remain underexplored. This review systematically categorizes these iron-based nanozymes, including iron oxides, single-atom enzymes, and metal–organic frameworks. We further elucidate their mechanisms in enhancing ferroptosis, focusing on their structural attributes, ROS generation pathways, and their enzymatic activities. Additionally, we summarized their biochemical applications alongside challenges in biosafety, nanozyme specificity, and advanced design and analysis approaches essential for maximizing their therapeutic efficacy.

[a]Department of Applied Biology and Chemical Technology, The Hong Kong Polytechnic University, Hung Hom, Kowloon, Hong Kong 999077, China. E-mail: jingjie.ge@polyu.edu.hk

[b]Sha Tin College, Fo Tan, New Territories, Hong Kong 999077, China

[c]Institute of New Energy for Vehicles, School of Material Science and Engineering, Tongji University, Shanghai 201804, P.R. China

† These authors contributed equally to this work.

Dr. Jingjie Ge is an Assistant Professor in the Department of Applied Biology and Chemical Technology at The Hong Kong Polytechnic University. She received her Ph.D. from the University of Science and Technology of China (USTC) in 2018. She then worked as a Postdoctoral Fellow and Research Assistant Professor at Nanyang Technological University and The Hong Kong University of Science and Technology, respectively. Her current research interests focus on atomic-level designing nanocatalysts and nanozymes for green chemistry and biology applications.

Jingjie Ge

1. Introduction

Malignant tumors, commonly referred to as cancer, pose a significant health threat worldwide. According to data from the Global Cancer Observatory, cancer was responsible for 22.8% of global deaths from noncommunicable diseases in 2022.[1] Traditional cancer treatments—such as surgery,[2] radiation therapy,[3] chemotherapy,[4] immunotherapy,[5] and targeted therapy[6]—are often associated with drawbacks. These include an increased risk of metastasis,[2] toxicity to normal tissues,[3] multidrug resistance,[4] immunosuppression,[5] and dependence on tumor heterogeneity.[6] Consequently, therapeutic strategies that induce selective cell death have garnered increasing attention recently.

Cell death is a vital biological process for mammalian development, homeostasis, and disease progression.[7] Traditionally, cell death is classified into three main types: apoptosis (type I), autophagy (type II), and necrosis (type III).[8] Recent research has refined this classification into two categories: accidental cell death (ACD) and regulated cell death (RCD). ACD occurs in response to uncontrolled chemical, physical, or mechanical stimuli, whereas pharmacological or genetic interventions can modulate RCD. RCD is subdivided into several major types, including necroptosis, pyroptosis, and ferroptosis.[9] However, studies have shown that DNA damage-induced apoptosis often proves ineffective due to specific genetic mutations (such as p53 mutations), contributing to drug resistance in certain chemotherapy treatments.[10] Given its critical role in tumor

suppression and its potential to overcome drug resistance, ferroptosis has garnered significant research interest as a therapeutic strategy for cancer treatment.[11,12]

Ferroptosis, an iron-dependent form of programmed cell death, was first proposed by Brent Stockwell and Scott J. Dixon in 2012.[13] This process is characterized by the accumulation of lipid peroxidation (LPO) induced by reactive oxygen species (ROS). A classical mechanism for ROS generation, Fenton chemistry, involves a redox reaction between Fe^{2+} and Fe^{3+}, producing hydroxyl radicals ($\cdot OH$).[14] LPO, ROS, and ferroptosis are closely interconnected in tumor therapy. Peroxidized lipids, which are key to ferroptosis, compromise the integrity of the cell membrane, ultimately leading to tumor cell death.[15] ROS, oxygen-derived radical species with unpaired electrons and high oxidative activity, are produced during redox reactions. As the primary inducers of LPO, ROS can oxidize polyunsaturated fatty acids, resulting in LPO accumulation and facilitating ferroptosis. Additionally, ROS can regulate the genome to promote ferroptosis.[16,17] Ferroptosis can be initiated through various pathways, including the suppression of Glutathione Peroxidase 4 (GPx4), inhibition of the FSP1-CoQ10-NAD(P)H pathway, and disruption of mitochondrial voltage-dependent anion channels.[8,14,18] Among these, GPx4 plays a crucial role in eliminating ROS and LPO at the tumor site by utilizing endogenous glutathione (GSH), thereby maintaining redox homeostasis within the tumor microenvironment (TME)[19,20] and inhibiting ferroptosis. Therefore, increasing ROS levels while depleting GSH to trigger tumor ferroptosis presents a promising therapeutic strategy.

ROS-mediated nanozyme therapy has recently gained significant attention in cancer treatment due to its ability to regulate oxidation reactions, ROS, and GSH simultaneously within the TME.[21–23] Nanozymes are nanomaterials that mimic the biocatalytic functions of natural enzymes. Since 2007, when Gao et al. first described the peroxidase (POD)-like activity of Fe_3O_4 nanoparticles,[24] the potential of nanomaterials as a catalyst to biological processes has been extensively studied. Notably, studies have shown that certain natural enzymes, such as ACLS4 and LPCAT3, regulate the intake of polyunsaturated fatty acids into cell membranes, thereby inducing LPO[25] and facilitating specific biological activities.[26] Nonetheless, natural enzymes, which are primarily based on biological materials, have several limitations. These include susceptibility to denaturation under harsh conditions, challenges in recycling, and high synthesis costs.[27–29] In contrast, nanozymes are favored by researchers due to their diverse enzymatic activities, excellent surface plasmon resonance (SPR) properties, photothermal conversion capability, and abundant antibody conjugation sites.[30] Its ability to modulate key metabolic pathways—such as iron metabolism, lipid metabolism, energy metabolism, and amino acid metabolism—allows nanozymes to enhance ferroptosis more efficiently than natural or artificial enzymes.[31–33]

Given the abundance of earth resources, low costs, and superior enzymatic performance of nanozymes, Fe-based nanozymes have been widely selected to mimic natural

enzymes for cancer therapy.[34–36] These include iron oxides,[37,38] iron-based single-atom enzymes (SAzymes),[39,40] and iron-based metal–organic frameworks (MOFs),[41,42] among others. It is well recognized that the ferric and ferrous sites within Fe-based nanozymes confer peroxidase (POD)-like activity by mimicking the active sites of the heme group in horseradish peroxidase (HRP).[24,34] Moreover, the excess iron in these nanozymes is able to enhance ROS production via the Fenton reaction whilst depleting GSH to reduce GPx4 expression, thereby promoting LPO and advancing ferroptosis.[43–45] Consequently, Fe-based nanozymes are emerging as promising candidates for tumor therapy. Researchers typically design iron-based nanozymes to enhance ROS generation and modulate the TME, emphasizing the importance of understanding the underlying mechanisms from the perspectives of cellular metabolism, immunology, and organelle damage induced by ferroptosis.[46–48] Hence, few systematic reviews comprehensively explore the mechanisms of ferroptosis induced by iron-based nanozymes from the perspective of redox substances in the TME.[49–51]

To address this gap, this review first categorizes various newly designed iron-based nanozymes, including iron oxides, iron-based single-atom nanozymes, and iron-based MOFs, along with illustrations of their active sites. Subsequently, by focusing on the redox substrates involved in the ferroptosis mechanism such as iron, LPO, and GSH, we summarize the role of ROS in cancer therapy and that of Fe-based nanozymes in the ferroptosis process via Fenton chemistry. This review also highlights the multiple enzymatic-like activities of Fe-based nanozymes, including POD-like activity, oxidase-like activity (OXD-like), glutathione oxidase-like activity (GSHOx), catalase-like activity (CAT-like), superoxide dismutase-like activity (SOD-like), and glucose oxidase-like activity (GOx-like). Moreover, we examine the corresponding ROS generation mechanisms of these nanozymes, emphasizing their latest biochemical applications. Finally, the challenges and prospects of advancing iron-based nanozymes for tumor therapy through ferroptosis will be discussed (Fig. 1).
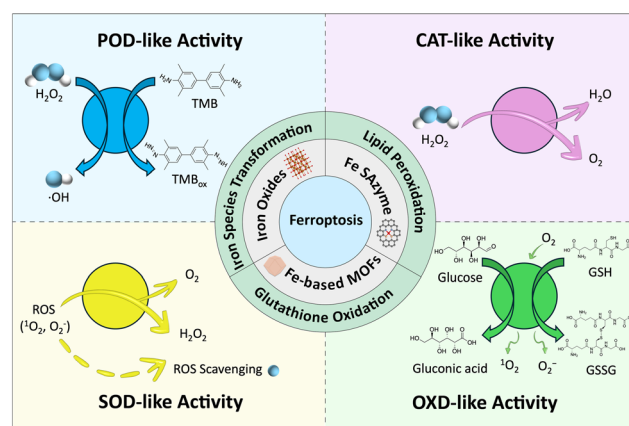

Fig. 1 Schematic illustration of ferroptosis enhanced by iron-based nanozyme.

2. Classification of iron-based nanozymes

The intrinsic biocatalytic activity of nanomaterials, specifically POD-like activity, was first studied in 2007 when Gao *et al.* discovered the inherent POD-like activity of Fe_3O_4 nanoparticles.[24] Since then, nanomaterials with biocatalytic activity have been referred to as nanozymes. It has been proven that iron is the most abundant and essential trace element in the human body.[24,52,53] Iron can both accept and donate electrons and is strongly associated with oxygen-related electron transfer processes and the metabolism of vital substances, hence it has significant biological importance. Subsequently, iron has been extensively investigated to construct various nanozymes, including iron oxides, iron-based SAzymes, iron-based MOF materials, *etc.* These iron-based nanozymes are designed to exhibit multiple enzymatic activities and enhance the generation of ROS, thereby boosting ferroptosis for tumor therapy.

Due to their relatively legible structures, the enzymatic activities of iron-based nanozymes can be optimized by regulating their size, crystalline structure, morphology, coordination environment, electronic structure, *etc.*[54] As a typical example, compared to natural enzymes, Fe SAzymes with similar Fe-Nx active sites have been proved to possess a simplified synthesis and purification method and a wider operation range.[55] However, limited by their randomly dispersed active sites, the SAzymes' specific enzymatic activity would be affected. Herein, the approaches for regulating their properties and related enzymatic activities of Fe-based nanozymes are systematically reviewed in this section.

2.1. Iron oxide

Monometallic iron oxides, such as hematite and magnetite, iron hydroxides, and iron oxide hydroxides, are materials with great application potential in tumor therapy.[56,57] The comparatively simple composition and crystal structure facilitates the preparation and analysis of the structure and function of these nanozymes. The physicochemical properties of nanozymes, including size, morphology, and facets, can greatly influence the dynamics of the Fenton reaction by altering the reaction metabolism and pathways.[58] Therefore, modulating these properties within nanozymes is crucial to optimize their enzymatic activity. Yin *et al.* designed an α-Fe_2O_3 nanosheet with a predominant (311) facet to enhance POD-like activity.[59] The schematic demonstration of the catalytic mechanism is shown in Fig. 2a. They examined the adsorption energy of H_2O_2 on different facets and the corresponding H_2O_2 activation energy barriers. Among the facets, the (311) facet showed the highest adsorption energy and the lowest activation energy barrier. This indicates a strong tendency for H_2O_2 adsorption and provides the most favorable pathway to convert H_2O_2 into •OH, thus facilitating the initiation of POD-like activity. The ability to generate •OH from H_2O_2 depicts its promising ability in pollutant depletion and LPO and GSH consumption, thus demonstrating its intrinsic ferroptosis-initiating potential.
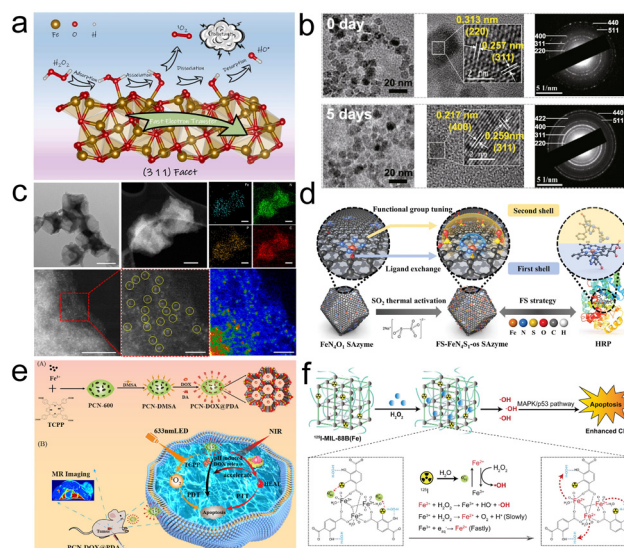

Fig. 2 (a) Illustration of the mechanism of POD-like activity of α-Fe_2O_3 with (311) facet.[59] Reproduced from ref. 59 with permission from Elsevier, Copyright 2024 (b) TEM, HRTEM and SAED images of Fe_3O_4 nanoparticles before and after catalysis.[60] Reproduced from ref. 60 with permission from Springer Nature, Copyright 2022 (c) TEM, HAADF-STEM and EDS mapping image of FeN_3P nanozyme.[67] Reproduced from ref. 67 with permission from Springer Nature, Copyright 2021 (d) schematic view of the synthesis of the FS-FeN_4S_1-os SAzyme.[69] Reproduced from ref. 69 with permission from Wiley-VCH, Copyright 2024 (e) schematic view of tumor therapy using PCN-DOX@PDA.[77] Reproduced from ref. 77 with permission from American Chemical Society, Copyright 2024 (f) ^{125}I enhanced Fenton reaction.[82] Reproduced from ref. 82 with permission from Wiley-VCH, Copyright 2024.

Dong *et al.* prepared Fe_3O_4 nanoparticles to analyze the catalytic mechanism of POD-like activity of the nanoparticles.[60] They discovered that the persistent catalytic activity of magnetite nanoparticles is achieved through the following processes. Primarily, a Fenton-like reaction occurs on the surface of the nanozyme, producing •OH by the decomposition of H_2O_2, while external Fe^{2+} is oxidized to Fe^{3+}. Concurrently, internal Fe^{2+} transfers electrons to the outer surface Fe^{3+} *via* the Fe^{2+}–O–Fe^{3+} chain, reducing surface Fe^{3+} and resulting in the migration of inner lattice Fe^{3+} to the surface. Once inner Fe^{2+} is depleted, the magnetite nanoparticles would transform into γ-Fe_2O_3. As shown in Fig. 2b, the lattice of Fe_3O_4 nanozymes undergoes structural changes during the catalytic process. Their research elucidates the underlying principles of Fe_3O_4 nanozyme inactivation and identifies the ion migration process as the rate-limiting step of the POD-like activity. This theory could serve as a foundation for the future design of Fe_3O_4 nanozymes.

Bimetallic oxides refer to a type of complex oxide containing two different metal elements. Compared to single iron oxide, an iron oxide that is composed of other metal oxides shows better enzymatic activity due to improvements in oxygen defects or valence state modulation.[61] Therefore, designing complex bimetallic oxides is a promising pathway toward enhancing tumor therapy. Yin *et al.* prepared a $MnFe_2O_4$-based

nanozyme coated with MOF to enhance the production efficiency of $^1O_2$ under photodynamic conditions.[62] The MOF coating not only improves the photosensitive ability of the nanozyme but also facilitates the diffusion of H_2O_2. The cascade enzymatic activity relies on the electron transfer ability of a multi-valence state metal oxide center, e.g., the conversion between Fe^{2+} and Fe^{3+} in Fenton-like reactions and the oxidation of GSH to GSSG. In vivo tumor suppression results suggested that the antitumor ability of the experimental group with laser radiation exhibited the best result relative to the non-irradiated control group.

The presence of oxygen defects on bimetallic iron oxides can also contribute to the enzymatic activity of the nanozyme. For example, $FeWO_x$ with surface oxygen defects demonstrates substantially higher catalytic activity than the original $FeWO_4$ without oxygen defects.[63] This enhancement stems from the increased exposure of iron ions on the surface of the nanozyme with oxygen vacancy sites, which formed during the synthetic processes through W^{6+} reduction. The authors declared that the intrinsic POD-like activity of this nanozyme enables its application in cancer sensing via photoacoustic imaging. Herein, the $FeWO_x$ bimetallic oxide nanozyme exhibits potential in tumor treatment due to its inherent Peroxidase-like activity.

Efficient cellular delivery of inorganic iron oxide nanozymes remains challenging for enhancing in vivo tumor therapy. Surface modification of nanozymes can not only affect the cell affinity of nanozymes but also improve the enzymatic activity of nanozymes.[64] For example, Chen et al. designed a FeOOH-based nanozyme modified with glutamine (Gln) and cellular uptake enhancer V9302 to test the effect of modification on cell uptake for enhanced pancreatic cancer treatment. The modified nanozyme demonstrated desirable ferroptosis-induced tumor suppression, compared to the primitive FeOOH material without Gln coating.[65]

2.2. Iron-based single-atom enzymes

Iron-based SAzyme is a type of artificial enzyme that constructs a single-atom iron onto metal oxides, metal sulfides, and carbon–nitrogen-based supplementary frameworks.[66] With a similar $Fe-N_x$ coordination structure to the natural enzyme, Fe SAzyme shows a strong Fenton response, thus generating plentiful ROS and exhibiting good therapeutic activity.[52] Compared to iron oxide nanozymes, Fe SAzymes can accomplish enzymatic activities with a significantly lower metal content. Besides, it is easier to regulate the active sites of single-atom metals in SAzymes by introducing multiple substances into the supplementary framework. For example, Ji et al. introduced poly-(cyclotriphospazene-co-4,4′-diaminodiphenylether) (PZM) during synthesis to both coordinate with the metal center and regulate the coordination structure.[67] As shown in Fig. 2c, the high-angle annular dark-field scanning transmission electron microscopy (HAADF-STEM) result and energy-dispersive X-ray spectroscopy (EDS) mapping demonstrate the uniform P atom distribution in the FeN_3P nanozyme. Compared to the porphyrin-like FeN_4C_4 structure on the traditional $Fe-N_4$ co-

ordinated SAN, the FeN_3PC_4 structure shows reduced electron transfer from Fe to N due to the electron donation effect of the phosphorus atom. This advancement has led to progress in the POD-like activity compared to Fe_3O_4 (111) and $Fe-N_4$ co-ordinated nanozyme.

Sulfur is also an ideal element for enhancing iron-based enzymatic activity. Iron–sulfur (Fe–S) structures in natural enzymes, essential for redox reactions in cell metabolism, have inspired the development of Fe–S-containing nanozymes to enhance multiple enzymatic-like activities, with dehydrogenases, hydrogenases, and certain monooxygenases being explored by researchers.[68] Choi et al. synthesized $Fe-N_4$ single-atom nanozymes with different ligand coordination: oxygen, sulfur without functional group, and sulfur with reduced and oxidized functional groups.[69] The synthetic method of the nanozyme is labelled in Fig. 2d. They revealed that adding reduced and oxidized sulfur ligands to $Fe-N_4$ SAzymes induced a second-shell coordination modification, thereby optimizing the electronic and geometric structures. Density functional theory (DFT) calculations revealed that this reduced the energy barrier of the intermediate steps for the Fenton-like reaction, thereby enhancing the POD-like activity. They also examined the cytotoxicity of the SAzymes based on different cancer cell lines, given that the H_2O_2 concentration in cancer cells is significantly higher than that in normal cells. The in vitro and in vivo tumor cell cytotoxicity analysis results showed that, while ZIF-NC showed little cytotoxicity across all concentrations, the sulfur-modified nanozymes exhibited strong antitumor ability in both in vivo and in vitro analysis.

Furthermore, by introducing heteroatoms into iron-based SAzymes, the electronic structure of the metal active site center in SAzymes can be tuned, thereby improving their affinity to substrates.[70] For example, Zeng et al. introduced Mn single atoms into the iron-based nanozyme, fabricating a dual-atomic Fe–Mn enzyme that successfully tunes the iron atom's D-band center.[71] According to the DFT calculations, compared to that of the Fe_1-NC_e single-atom catalyst, the D-band center of the $Fe_1-Mn_1-NC_e$ dual-atom nanozyme is closer to the Fermi level. Regarding the change in POD-like activity, $Fe_1-Mn_1-NC_e$ shows a stronger affinity between the iron single atom and H_2O_2, resulting in enhanced enzymatic activity compared to Fe_1-NC_e single atom nanozyme.

The selectivity of multiple enzymatic activities in nanozymes is crucial for applications in tumor therapy. Zhang et al. discovered that by tuning the distance between neighboring iron single atoms in an iron single-atom nanozyme, the selectivity of CAT-like activity over POD-like activity would improve significantly.[72] The authors argue that the adjacent activation centers of Fe_2-SAzyme reduce the free energy for the rate-determining step by facilitating the end-bridge adsorption of H_2O_2 on the nanozyme. In contrast, the end-on adsorption mechanism of traditional Fe-SAzyme exhibits a higher free energy for the rate-determining step. A similar observation has been proposed for neighboring M_2-SAzymes (Pt, Ir). Their work offers insight into enhancing the enzymatic selectivity of nanozymes via the active site modification.

2.3. Iron-based MOFs

Metal–organic frameworks (MOF), composed of metal nodes and organic ligands, are characterized by their design-functional adaptive structure, intelligent release capability, large specific area contributed by their porous structure, stimuli-response ability and drug-delivery ability compared to activated carbon material and organic carriers.[73–76] Like single-atom nanozymes, iron-based MOFs also possess single iron atoms that act as the catalytic center for enhanced catalytic activity, however, MOF materials possess more biotic proficiency, demonstrating its better potential in clinical applications.[74] Due to its adjustable pore size, high selectivity, and large surface area, iron-based MOFs can carry metal ions and drug molecules to targeted sites, thereby enhancing anti-tumor ability. Chen et al. designed an iron-based MOF by coordinating Fe^{3+} with a porphyrin-like ligand, assembled with doxorubicin (DOX) and modified with polydopamine (PDA), to produce PCN-DOX@PDA.[77] Fig. 2e presents a schematic illustration of the mode of action for PCN-DOX@PDA. They analyzed the photothermal effect of the material along with the release of DOX under different pH values and photothermal conditions. The results show that the decomposition of PDA occurs either at pH = 5.4 or with NIR light treatment, suggesting that the synthesized material can intelligently release antitumor drugs. Additionally, the fluorescence results from confocal laser scanning microscopy (CLSM) revealed that the PCN@PDA material can generate ROS when exposed to an LED.

Loading MOF materials with multiple enzymes could be an effective way to design cascade nanozymes for cancer therapy.[78] For example, Fang et al. designed a Co-ferrocene MOF loaded with GOx(Co-Fc@GOx) to analyze cascade enzymatic activity with potential applications in tumor treatment.[79] The synthesized material exhibits a desired Fenton effect in the absence of GOx, while its cascade enzymatic activity is determined by the TMB colorimetric reaction in an aqueous glucose solution. Furthermore, the bio-experiment results confirm the enhanced in vivo antitumor efficacy.

MOF materials can also be modified to enhance the reduction of metal nodes, thereby increasing the efficiency of chemodynamic therapy (CDT), photodynamic therapy, sonodynamic therapy (SDT), and magnetodynamic therapy (MDT).[74,80,81] By introducing a radioactive isotope (^{125}I) into an iron-based MOF, Wang et al. proposed a novel synergistic MOF material for enhanced POD-like activity.[82] As shown in Fig. 2f, they suggested that ^{125}I can generate hydrated electrons in an aqueous environment, which can then facilitate the reaction from Fe^{3+} to Fe^{2+}. The continuous supply of Fe^{2+}, through the conversion of Fe^{3+}, significantly enhances the tumor treatment efficiency of ^{125}I-MIL-88B (Fe) compared to both ^{125}I-doped SiO_2 and MIL-88B (Fe). This improvement highlights a synergistic effect in enhancing chemodynamic therapy.

Iron-based MOFs, capable of carrying monomeric compounds, can enhance CDT and be combined with immunotherapy to induce ferroptosis more effectively.[83] Li et al.

designed a MIL-101 (Fe) based MOF material loaded with dihydroartemisinin (DHA), which reprograms tumor-associated macrophages (TAMs) into an anti-tumor M1 phenotype via ferroptosis, thereby improving tumor therapy.[84] The integration of DHA with MOF not only increases the hydrophilicity and targeting accuracy of DHA in vivo, but also promotes the generation of LPO, ROS, and iron ions through MIL-101 degradation in acidic environments (pH = 5.2). Their work provides valuable insights into applying Fe MOF-based nanozymes in immunotherapy through ferroptosis induction.

Photodynamic therapy (PDT) has been recognized as an effective way of enhancing ROS generation and ferroptosis induction.[85] However, its tumor treatment efficiency is often restrained by the oxygen deficiency in TME. To address this limitation, MOF materials can be modified to uplift photocatalytic generation of dioxygen molecules (O_2) in vivo, thereby enhancing the induction of ferroptosis through membrane LPO. Following this theory, Xu et al. designed a multifunctional nanocomplex for effective tumor PDT.[86] By modifying an iron-based MOF (MIL-53) with cMBP peptide, ferroptosis inducer sorafenib tosylate (ST), and photosensitizer Chlorin e6 (Ce6), the synthesized MIL-53@cMBP@ST/Ce6 (MMSC) nanozyme exhibits desired multiple enzymatic activities, including the oxidation of GSH together with POD-like and CAT-like activity. The enhancement of ferroptosis inducement under PDT was confirmed using a ferroptosis inhibitor, and cell viability analysis of MMSC treatment demonstrated a significant difference in treatment outcomes when exposed to varying laser intensities. Their research offers an innovative strategy for increasing O_2 generation to enhance ferroptosis.

SDT applies ultrasound (US) irradiation to develop sonosensitizer-mediated serve technology that is based on PDT.[81] Iron-based MOF nanozymes serve as important sonosensitizers that can be activated by US irradiation to generate ROS, thereby enhancing ferroptosis. Cao et al. constructed a Fe-MOF carrying Mn_2O_3 (FTM@AM) for enhanced treatment of triple-negative breast cancer (TNBC) by SDT.[87] The evaluation of ˙OH generation by Fenton reaction under US irradiation has been proved to increase by 33.8% compared to the control group with no US irradiation applied. The in vivo antitumor ability analysis of FTM@AM with the US and buffer solution shows that the tumor growth inhibition rate decreased by 93.6% compared to the control group. The results indicate that MOF-involved SDT leverages iron-based nanozymes to amplify ultrasound-triggered ROS generation through enhanced Fenton reactivity and ferroptosis synergy, achieving superior antitumor efficacy with targeted therapeutic precision.

MDT is a crucial measure for in vivo tumor detection and tumor therapy. Introducing iron MOF-based nanozymes in tumors could significantly enhance magnetic resonance imaging (MRI) signals due to their accumulation in tumor sites.[88] Yuan et al. explored the enhanced POD-like activity of magnetic nanozymes under a magnetic field.[74] They assembled a porphyrin-based Zr-MOF (PCN) on zinc ferrite (ZF) nanoparticles to produce a MOF-based magnetic nanozyme (PZFH) and reviewed the change in POD-like activity in

response to varying magnetic field intensities. Their findings revealed that with increasing magnetic field intensity, the POD-like enzymatic kinetics increased significantly. Herein, the connection between magnetically responsive nanozymes and tumor detection and therapy is established, inspiring future research on MDT-based treatments.

3. Mechanism of Fe-based nanozymes enhanced ferroptosis

Nowadays, recent studies have demonstrated that ferroptosis acts as a tumor suppressor by eliminating damaged or nutrient-deprived cells. It plays a crucial role in key tumor suppressor pathways, with its sensitivity being influenced by the activities of p53 and KEAP1/NRF2.[7,89–91] Among them, as one of the most extensively studied tumor suppressor genes, p53 positively regulates the ferroptosis pathway by transcriptionally repressing the expression of the cystine/glutamate antiporter. Intracellular iron can be exported *via* the iron transporter protein (FPN), which is the only known iron exporter in mammals that controls iron efflux.[92–94] Increased iron uptake or reduced iron export can make cancer cells more sensitive to oxidative damage and ferroptosis.[95]

At the molecular level, lipid peroxides are further decomposed into reactive substances that can deplete nucleic acids and proteins, leading to cell death by ferroptosis. LPO mediated by iron-containing enzymes, such as arachidonic acid lipoxygenases (ALOXs), is a primary mechanism. The small scaffold protein Raf1 kinase inhibitory protein (RKIP1) actively regulates ferroptosis by binding to lipoxygenase ALOX15 and interfering with the production of phosphatidylinositol.[96,97]

Reduced GSH is synthesized in two steps from glutamate, cysteine, and glycine in the cytosol, catalyzed by the enzymes glutamate-cysteine ligase (GCL) and glutathione synthetase (GSS).[98] It is the primary antioxidant in mammalian cells. Ferroptosis is deeply related to GSH depletion, either by blocking the uptake of cystine from the extracellular environment or inhibiting GSH biosynthesis. For instance, erastin inhibits system Xc- (one of the transporters that exerts the exchange of cystine and glutamate across plasma membrane) and buthionine sulfoximine (BSO) can inhibit γ-glutamylcysteine synthetase.[94]

Additionally, in cancer immunotherapy, ferroptosis is implicated in T cells and interferon-gamma (IFNγ)-mediated tumor suppression. Enhancing dietary intake of polyunsaturated fatty acids (PUFAs) or iron can increase the susceptibility of tumor cells to the pro-ferroptotic effects of CD8+-T cell-dependent immune therapy.[99,100]

Fe-based nanozymes can serve as ideal mediators, effectively linking oxidation reactions with ROS, thereby enhancing the efficiency of ferroptosis. During the ferroptosis process of tumor cells, key physiological changes include an increase in iron ions and ROS levels, excessive accumulation of LPO, and the inactivation or suppression of GPx4, as GSH is eliminated.[18,101] The oxidative stress pathway is widely recog-

nized as a fundamental causal component of ferroptosis and plays a crucial role in the interplay among these three substances.[80] In this section, the specific mechanisms within ferroptosis mediated by iron-based nanozymes will be discussed, focusing particularly on the redox substrates involving iron, LPO, and GSH.

3.1. Iron species transformation *via* Fenton chemistry

Fenton/Fenton-like reactions were first put forward by Henry J. Fenton in the 1890s,[102] as can be seen in Fig. 3a. The reactions mainly refer to the cycle of Fe^{3+} to Fe^{2+} ions alongside the accompanied generation of ROS during the process. It was previously thought that iron-based nanomaterials induced apoptosis by releasing Fe^{2+} ions from exposed nanoparticles into the surrounding solution. This process was believed to increase intracellular iron levels through endocytosis, ultimately leading to the production of •OH *via* the Fenton reaction. With a deep investigation into the intraparticle electron transport process, Yi *et al.* found out that the presence of internal low-valence iron (Fe^0 and Fe^{2+}) in Wüstite (FeO) nanoparticles can facilitate the transformation of Fe^{3+} into Fe^{2+} ions, thereby elevating the overall catalytic activity and increasing the intracellular ROS level in mouse mammary carcinoma cells.[103] Consequently, the redox cycle between the different iron species plays a critical role in the Fenton reaction, as shown in Fig. 3b. To boost the transformation of Fe^{3+} into Fe^{2+}
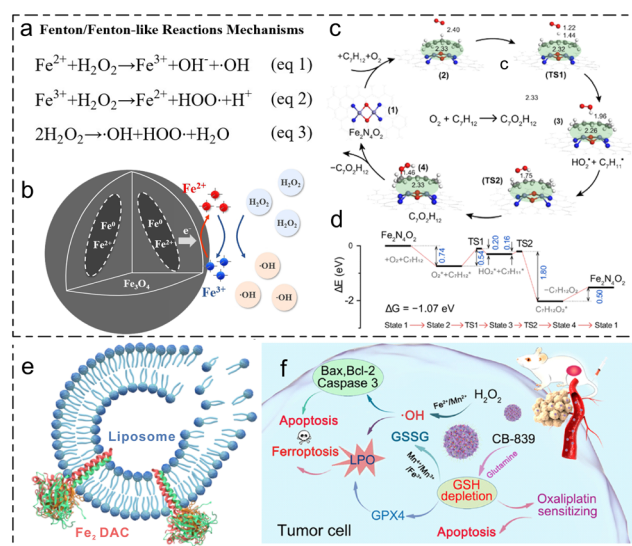

Fig. 3 Mechanism of Fe-based nanozymes enhanced ferroptosis. (a) The Fenton/Fenton-like reaction mechanisms. (b) Schematic diagram of enhancing surface Fenton reaction *via* intraparticle electron transport.[103] Reproduced from ref. 103 with permission from Wiley-VCH, Copyright 2023 (c) and (d) Gibbs free energy profile for key intermediate and transition states in the LPO cycle. Energy unit: eV.[113] (e) Schematic illustration of lipid destruction upon treatment with Fe₂ dual atom catalysts.[113] Reproduced from ref. 113 with permission from Springer Nature, Copyright 2023 (f) mechanism of DFMC nanoplatform with dual-GSH consumption characteristics and POD-like enzyme activity.[121] Reproduced from ref. 121 with permission from American Chemical Society, Copyright 2022.

during ferroptosis, Zhang *et al.* put forward an X-ray-activated Fe^{2+} supply platform which comprised of a $CaWO_4$ core and surface-decorated Fe_3O_4, to enhance tumor ferroptosis.[104] Upon X-ray irradiation, the ultraviolet light emitted by the $CaWO_4$ catalyzed the reduction of Fe^{3+} to Fe^{2+}, hence initiating a Fenton reaction cascade that produces highly toxic •OH. Moreover, to enhance the cycling of Fe^{2+} and Fe^{3+}, Shi and his group recently designed an allicin-modified $FeO_{1-x}OH$ nanozyme with varied iron valence states (Fe^{2+} and Fe^{3+}).[105] The high levels of reduced GSH in TME promote the reduction of Fe^{3+} to Fe^{2+}, accelerating the Fenton reaction and thereby amplifying ferroptosis-based therapeutic effects. In summary, optimizing the Fe^{3+} and Fe^{2+} transformation pathways can overcome the rate-limiting steps in Fenton chemistry. By introducing external energy sources and leveraging GSH inside the tumor, researchers can design iron-based nanozymes with enhanced ferroptosis efficiency.

Moreover, despite the extensively used H_2O_2, other peroxides, including artesunate (ART) have been proven as the optional link between Fe^{2+}/Fe^{3+} and ROS. Chen *et al.* utilized ART as a non-Fenton-type substrate to generate free radicals by ferrous ions intratumor.[106] The mechanism involves the decomposition of ART's endoperoxide bridges, which is catalyzed by ferrous ions (Fe^{2+}) and accompanied by the production of superoxide anions ($•O_2^-$). This targeted release further enhanced the chemo-dynamic therapy (CDT) effect within the tumor.

3.2. Lipid peroxidation (LPO) *via* Fenton chemistry

As the key biomarker for assessing susceptibility to ferroptosis, LPO refers to a complex process of lipid metabolism, which involves an enzymatic reaction and a nonenzymatic Fenton reaction pathway.[7,107,108] During the iron-based nanozymes-mediated Fenton process in tumor cells, accumulated ROS react with polyunsaturated fatty acids (PUFAs) side chains in phospholipids, membrane receptors, and macromolecules to oxidize biological membranes.[109] This LPO reaction results in the formation of LPO, such as malondialdehyde (MDA) and 4-hydroxynonenal (HNE). Ultimately, the fluidity and permeability of the cell membrane are altered, leading to changes in cell structure and inducing tumor cell death.[110,111]

Zhu *et al.* synthesized a metal-phenolic nanocatalyst containing ferric ions (Fe^{3+}) and mitoxantrone (MT, a kind of chemotherapeutic drug) in a self-assembled reaction.[112] Upon internalization by tumor cells, the fabricated nanoplatform can release MT to promote irreversible ferroptosis by increasing ROS-sensitive PUFAs and inducing lethal LPO. To further reveal the mechanism of LPO, Li and his group prepared a diatomic iron nanozyme, as illustrated schematically in Fig. 3e.[113] The Fe–O–Fe motif effectively aligns the energy levels of the Fe_2 minority β-spin d orbitals with the π* orbitals of the pentadiene moiety in vesicle membranes. This alignment significantly lowers the activation barrier for the reaction (Fig. 3e). Therefore, designing Fe-based nanozymes that incorporate LPO-sensitive drugs can enhance LPO efficiency during tumor therapy. Additionally, by regulating the structure and coordination environment of the iron center, the activation energy between the catalysts and lipid membranes can be lowered, optimizing therapeutic outcomes.

Iron-based nanozymes selectively target LPO processes in tumor cells by leveraging their unique catalytic properties and interactions with cellular components. Zhou *et al.* designed a kind of DNA nanozyme to enhance targeting delivery and induce ferroptosis within the tumor by incorporating hemin, an iron-containing porphyrin cofactor, into its structure.[114] The DNA nanozyme was constructed using rolling circle amplification and contains repeated AS1411 G-quadruplex (G4) units. These G4 units serve as active ligands for targeted tumor delivery due to their high affinity for nucleolin, which is overexpressed on the surface of tumor cells,[115] thus facilitating the LPO accumulation and GSH depletion during the treatment. Another approach involves the use of lipoxygenase (LOX) and phospholipase A2 (PLA2) to enhance LPO and ferroptosis in tumor cells. Zhang *et al.* developed a FeCo/Fe–Co dual-metal atom nanozyme co-loaded with LOX and PLA2.[116] The upregulation of arachidonic acid (AA) expression through PLA2 catalysis can synergize with CD8+ T cell-derived IFN-γ to induce ACSL4-mediated immunogenic tumor ferroptosis. This process involves the incorporation of AA into membrane phospholipids, which then undergo peroxidation with the participation of LOX. In summary, iron-based nanozymes can be strategically designed by incorporating LPO-related enzymes or by being loaded onto highly biocompatible carriers to induce LPO, thereby achieving selective and effective cancer treatment.

3.3. Glutathione (GSH) oxidation *via* Fenton chemistry

GSH, a key low molecular thiol, plays a crucial role as a cofactor in detoxifying reactive LPO and reducing ROS in conjunction with GPx4, which contributes to a diminished ferroptosis effect.[117] Therefore, to depress the GPx4 pathway[118] and enhance ferroptosis, it is essential to deplete the GSH levels within the TME.[119,120] Interestingly, iron-based nanozymes can oxide GSH into oxidized glutathione (GSSG) *via* Fenton chemistry, while replenishing Fe^{2+} ions, which possess higher Fenton reaction activity (eqn (1)).[102]

$$Fe^{3+} + GSH \rightarrow Fe^{2+} + GSSG \text{ (glutathione disulfide)} \quad (1)$$
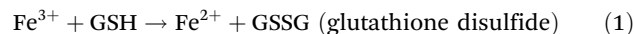
Yan and her group prepared pyrite peroxidase nanozymes that exhibit a self-cascade mechanism to generate abundant •OH while also depleting GSH. This effectively induces both apoptosis and ferroptosis in tumor cells.[45] By employing high-resolution mass spectrometry, it was revealed that the GSSG was generated from GSH during the catalytic process. Moreover, by mimicking the physiological environment of TME, pyrite nanozymes were able to maintain the selectivity of oxidizing GSH without interference from other compounds. Besides, Wu *et al.*[121] utilized Fe_3O_4 nanoparticles and CB-839 (a glutaminase inhibitor) to achieve a dual GSH depletion strategy for antitumor therapy. As shown in Fig. 3f, the Fe_3O_4 NPs facilitate the scavenging of GSH. Furthermore, CB-839 inhibits the synthesis of endogenous GSH by blocking gluta-

mine metabolism and reducing tumor cell drug resistance. Therefore, to enhance ferroptosis efficiency by targeting the GSH oxidation process, we could design Fe-based nanozymes with enhanced Fe^{3+} levels *via* valence regulation, implement a surface modification to improve GSH affinity, and incorporate compounds (such as GSH inhibitors) or synergistic metallic elements to augment effectiveness.

4. Iron-based enzyme-like activity

The enzymatic activity of nanozymes mainly involves the generation of ROS, which includes free radical species such as •OH, singlet oxygen ($^1O_2$), and $•O_2^-$, as well as non-radical molecules like H_2O_2, hypochlorous acid (HClO), and lipid peroxides (ROOH). Due to their unpaired electrons with high oxidative activity, ROS can interact with biological macromolecules such as DNA, proteins, and lipids, resulting in oxidative chain reactions that are closely related to oxidative stress damage, cellular aging, programmed cell death, and disease development.[122,123] The enzyme-like activities involved in iron-based nanozymes possess include POD-, OXD-, GSHOx-, CAT-, SOD-, and GOx-like activity. Herein, the relationship between various enzyme-like activities of iron-based nanozymes and ROS is summarized, thereby promoting the biocatalytic reaction of substrates.

4.1. POD-like activity

Peroxidase (POD) enzymes can catalyze the oxidation of H_2O_2 or organic peroxides with H_2O_2 as an electron acceptor, producing highly active intermediate species. Most natural POD enzymes refer to heme proteins.[124] Since 2007, when Gao *et al.* discovered that iron-containing magnetite nanoparticles (Fe_3O_4 NPs) exhibit similar activity,[24] there has been a surge of research focusing on the POD-like enzymatic activity of nanomaterials. There are two primary strategies for enhancing the POD-like activity of iron-based nanozymes: regulating the valence state of iron active sites and modifying the coordination environment of the metal active centers.

Wan *et al.* proposed a reaction pathway for the POD-like activity for Fe_3O_4 nanoparticles.[125] According to the result by DFT calculation, as shown in Fig. 4a and b, they argued that a $Fe^{IV}=O$ bond is present in the nanozyme structure because the Fe–O bond length was found to be 1.64 Å, which is an important intermediate for the generation of •OH. The analysis of POD-like activity under different redox substrate treatments also indicated that when Fe_3O_4 NPs are treated with oxidative species, *i.e.* $NaIO_3$, the POD-like activity is comparatively higher than those with and without $NaBH_4$ treatment.

Modifying the coordination environment of Fe SANs has proved to be a promising measure for enhancing the POD-like activity of nanozymes. Han *et al.* regulated the coordination structure of carbon-dot-supported iron single-atom nanozymes using phenanthroline to produce ph-CDs-Fe SAzyme.[126] Based on DFT calculation, the authors claim that, compared to CDs-
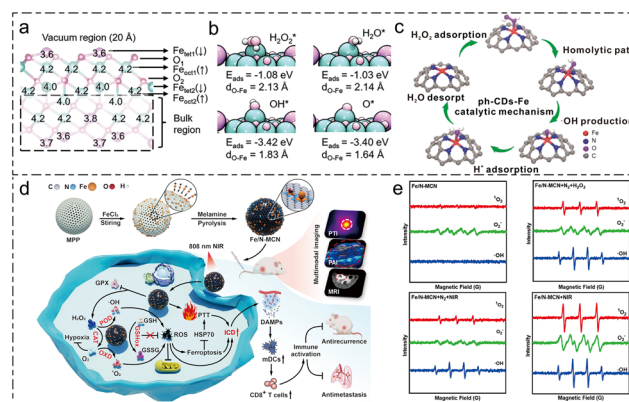

Fig. 4 Schematic review of POD-like activity and OXD-like activity. (a) The optimized structure of Fe_3O_4 (111).[125] (b) The adsorption structure, E_{ads} and d_{O-Fe} of $H_2O_2^*$, H_2O^*, OH^*, and O^*.[125] Reproduced from ref. 125 with permission from Wiley-VCH, Copyright 2022 (c) schematic illustration of the catalytic mechanism of ph-CDs-Fe.[126] Reproduced from ref. 126 with permission from Wiley-VCH, Copyright 2023 (d) schematic illustration of cascade enzymatic activity of Fe/N-MCN in enhancing ferroptosis.[132] (e) Electron spin resonance (ESR) spectra-measured $^1O_2$, $•O_2^-$ and •OH in different reaction conditions with/without the presence of O_2, H_2O_2 and NIR.[132] Reproduced from ref. 132 with permission from Elsevier, Copyright 2025.

Fe SAzyme, ph-CDs-Fe SAzyme possesses a higher ratio of pyrrolic N in the coordination structure. Moreover, the slightly protruding structure of Fe atoms on the surface of the nanozyme strengthens the adsorption effect of H_2O_2. As shown in Fig. 4c, the adsorption effect of H_2O_2 plays a crucial role in the POD-like activity of ph-CDs-Fe. Moreover, the enzyme kinetics data show a slight increase in H_2O_2 adsorption and an increase in V_{max} up to three times of ph-CDs-Fe SAzyme compared to CDs-Fe SAzyme.

For the selective enhancement of POD-like activity, Jiao *et al.* proposed a heteroatom-doping strategy on the carbon–nitrogen framework of FeNC single-atom nanozyme.[127] They applied X-ray photoelectron spectroscopy (XPS) to test the doping nature of boron in the nanozyme. The result of the enzymatic activity test shows that the POD-like activity of FeBNC is enhanced by 191.2%. In comparison, the CAT-like activity enhancement is only 11.9% compared to FeNC, indicating that the strategy of boron atom doping is effective for the selective enhancement of POD-like activity. They attributed the selective enhancement to the electronic structure rearrangement induced by heteroatom doping. They proposed that introducing B atoms could achieve an electron structure rearrangement of the center metal atom, thereby selectively enhancing the POD-like activity.

The quantitative analysis of POD-like activity for nanozymes involves three main factors: K_m, which evaluates the affinity of certain substrates to nanozymes; V_{max}, which describes the maximum velocity for enzymatic reactions; and k_{cat}/K_m, which is the specific constant of enzymatic kinetics. The specified kinetic data for several typical types of nanozymes as classified in this review are labelled below in Table 1.

Table 1 The comparison of POD-like activity kinetics of selected nanozymes

Nanozyme	Substrate	K_m (mM)	V_{max} (mM min^{-1})	k_{cat}/K_m (mM^{-1} min^{-1})
Fe$_3$O$_4$ NPs[125]	TMB	9.93	2.61×10^{-3}	5.25×10^2
	H$_2$O$_2$	0.92	2.55×10^{-6}	8.93×10^{-3}
FeWO$_x$ NSs[63]	TMB	0.03	7.35×10^{-3}	NA
	H$_2$O$_2$	3.26	0.261	NA
FeNC[127]	TMB	24.25	0.034	22.8
	H$_2$O$_2$	1.48	0.0329	1.80×10^2
FeBNC[127]	TMB	25.24	0.0109	3.04×10^3
	H$_2$O$_2$	2.22	0.0768	8.79×10^2
ph-CDs-Fe[126]	TMB	5.55×10^{-2}	1.11×10^{-2}	2.47
	H$_2$O$_2$	24	16.66	8.50
PZF unexposed to AMF[74]	H$_2$O$_2$	14.23	2.62×10^{-6}	2.79×10^{-3}
PZF exposed to AMF[74]	H$_2$O$_2$	13.98	1.29×10^{-5}	1.40×10^{-2}
D/P@ZUCO[128]	H$_2$O$_2$	1.06×10^{-3}	8.36×10^{-3}	NA
HRP[24] (Fe species)	TMB	0.434	6.00×10^{-3}	5.53×10^5
	H$_2$O$_2$	3.70	5.23×10^{-3}	5.64×10^4

4.2. OXD-like activity

Oxidase-mediated catalytic decomposition reactions generally refer to redox reactions involving O$_2$. These reactions can oxidize O$_2$ into ROS such as H$_2$O$_2$, ^{1}O$_2$, or •O$_2^-$. These ROS can further react with GSH or lipid species, thereby depleting GSH and generating LPO to promote ferroptosis. Notably, this family of enzyme activities also includes GSHOx-like and GOx-like activities.[129]

4.2.1. •O$_2^-$ participated in OXD-like activity. The generation of •O$_2^-$ results in cytotoxic effects, as these ROS can interact with and damage various biomolecules, including lipids, proteins, and nucleic acids.[130] •O$_2^-$ species can serve as precursors for generating H$_2$O$_2$, which produces •OH either by Fenton reactions or decomposition reactions by POD-like nanozymes.
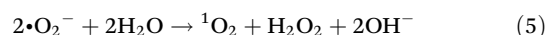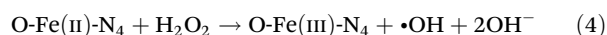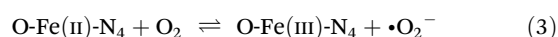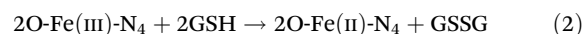
Li et al. utilized the oxidase-like (OXD) enzymatic activity of tetranitro iron phthalocyanine (TNFe(II)Pc) to oxidatively treat phenol and chlorophenol-contaminated water.[131] They were the first to propose a reaction process involving •O$_2^-$, suggesting that the formation of •O$_2^-$ and the degradation of these phenolic substrates resulted from the substrates continuously transferring single electrons to O$_2$. Building on this work, Qin et al. explored the OXD-like activity of catalyzing dissolved O$_2$ into •O$_2^-$ for the enhancement of ferroptosis.[132] The electron spin resonance (ESR) spectra displayed in Fig. 4e reveal distinct characteristic peaks for ^{1}O$_2$ and •O$_2^-$. Their findings indicate that the catalytic activity of TMB oxidation is enhanced under 100% dissolved oxygen level but inhibited in N$_2$ atmosphere. The antitumor ability shown in Fig. 4d is assessed regarding the cascade enzymatic activity. The results of the in vitro cell viability test demonstrate that, with the progression of near-infrared (NIR) irradiation, Fe/N-MCN exhibits superior tumor inhibition ability as a nanozyme. The in vivo assessment of the antitumor ability of Fe-N/MCN of MCF-7 and 4T1 bearing mice shows that with NIR irradiation, Fe-N/MCN can not only inhibit the growth of in situ breast tumor but can also suppess the distal metastasis of the tumor to lung and liver.

4.2.2. ^{1}O$_2$ participated in OXD-like activity. Unlike •O$_2^-$, ^{1}O$_2$ can react directly with lipids to cause LPO, thereby dama-

ging the cell membrane and producing LPO.[133] The generation of ^{1}O$_2$ involves the participation of a photosensitizer, light irradiation, and molecular oxygen, in which the O$_2$ molecules is converted to bioactive ^{1}O$_2$ via a light-induced transition involving energy transfer from the photosensitizer.[134]

Feng et al. designed an iron single-atom nanozyme (FeSA-OLC) by calcinating Fe(phen)$_x$ with an onion-like carbon support.[135] The catalytic product of OXD-like activity is characterized. ESR results show distinctive resonance peaks for both ^{1}O$_2$ and •O$_2^-$ in the reaction system, demonstrating the details for the intermediate steps of the O$_2$ present catalysis of TMB oxidation. Their results also indicate that the generation of ^{1}O$_2$ and •O$_2^-$ is temperature-dependent.

The coordination structure of OXD-mimicking nanozyme can affect OXD-like activity. Liu et al. synthesized an axial O atom-modulated Fe(III)N$_4$ nanozyme. The reaction formulas of OXD-like catalytic activity are labelled below.

$$2\text{O-Fe(III)-N}_4 + 2\text{GSH} \rightarrow 2\text{O-Fe(II)-N}_4 + \text{GSSG} \quad (2)$$

$$\text{O-Fe(II)-N}_4 + \text{O}_2 \rightleftharpoons \text{O-Fe(III)-N}_4 + \bullet\text{O}_2^- \quad (3)$$

$$\text{O-Fe(II)-N}_4 + \text{H}_2\text{O}_2 \rightarrow \text{O-Fe(III)-N}_4 + \bullet\text{OH} + 2\text{OH}^- \quad (4)$$

$$2\bullet\text{O}_2^- + 2\text{H}_2\text{O} \rightarrow {}^1\text{O}_2 + \text{H}_2\text{O}_2 + 2\text{OH}^- \quad (5)$$

Its catalytic reaction process was evaluated by DFT calculations.[136] It revealed that, by anchoring an axial oxygen atom on the FeN$_4$ active site, the symmetrical structure of the active site broke, causing the d-band center to approach the Fermi level. The tumor inhibition of the nanozyme was also evaluated. The in vivo tumor growth inhibition (TGI) rate of the material was measured to be 86.1%. Thanks to this remarkable TGI rate, the survival period of mice treated with O–Fe-N$_4$ extended up to 55 days.

4.2.3. GSHOx-like activity (GSH involved in OXD-like activity). GSH is an intracellular peptide primarily involved in detoxification, free radical scavenging, antioxidation, and regulation of key cellular processes such as DNA synthesis and immune function.[137] In the presence of GSH peroxidase, GSH reduces ROS that cause LPO and cellular damage to prevent

physiological oxidative stress damage in the mitochondria. However, to maintain homeostasis and balance ROS accumulation, tumor cells often counteract by increasing intracellular GSH levels (approximately four times that of normal cells). This elevated GSH content can lead to an efflux of Pt-based chemotherapeutic drugs from cells, leading to drug resistance. Additionally, it hinders the use of nanozyme platforms that introduce external ROS for mediated therapy.[137] Therefore, research on strategies to promote intracellular GSH depletion to modulate the tumor microenvironment (TME) has surged, aiming for more effective catalytic therapy.[118,138]

Fan *et al.* synthesized Fe-TCPP MOFs and explored their responsiveness to GSH.[139] By analyzing the color change and the fluorescence signal intensity of GSH-incorporated Fe-MOF-RP solution, they observed a GSH concentration-dependent reduction in fluorescence intensity, accompanied by a notable color change as demonstrated in Fig. 5a. This indicates that a redox reaction between GSH and Fe^{3+} has taken place, leading to the oxidative consumption of GSH. They further evaluated the antitumor effect of Fe-TCPP MOF with

laser on mice with melanoma with distal lung metastasis. The *in vivo* antitumor assessment shows good results induced by triggering a strong immune response with GSH depletion in tumor sites.

Besides being oxidized with the involvement of O_2, GSH can also be oxidized with the presence of H_2O_2 or organic peroxides. Wu *et al.* characterized the ability to oxidize GSH of synthesized Fe_3S_4 nanozyme in the presence of H_2O_2 by DTNB (5,5′-dithiobis (2-nitrobenzoic acid)) colorimetry assessment.[140] The color change of DTNB is analyzed by measuring the absorption peak at 412 nm, which corresponds to the typical absorption peak of the reaction product between GSH and DTNB. The addition of Fe_3S_4 nanozyme resulted in a significant decrease in the absorption value, suggesting that the catalytic reaction between Fe_3S_4 nanozyme and GSH was effectively carried out. The antitumor effect assessment displayed in Fig. 5b illustrates the superior antitumor ability of Fe_3S_4 nanozyme compared to the control group.

4.2.4. GOx-like activity (glucose involved in OXD-like activity).
Glucose is an essential substance in tumor metabolism. Via aerobic glycolysis, glucose can be converted into the basis for cellular compounds, *e.g.* NADPH and ATP.[141] Nanozymes with GOx-like activity can effectively promote glucose consumption by decomposing glucose into gluconic acid and H_2O_2.[142] The depletion of glucose by GOX-mimicking nanozymes can also trigger hunger-induced apoptosis, and the produced H_2O_2 is also involved in other enzymatic reactions that trigger ferroptosis-induced cell death. The iron-based nanozyme modified with GOx-mimicking nanocatalysts can effectively enhance the nanozyme's cascade enzymatic activity to enhance the effects of tumor therapy.

One effective measure to achieve tandem enzymatic activity is to modify MOF materials with the natural GOx enzyme.[143] Liu *et al.* designed an ultrathin 2D Cu-TCPP (Fe) MOF with GOx adsorption to convert glucose into gluconic acid and H_2O_2, thereby promoting the production of highly toxic •OH groups.[131] Another newly developed method for cascade enzymatic activity design involves attaching artificial GOx mimics, *i.e.,* Au nanoparticles, to iron-based nanozymes. By attaching Au NPs to Fe_2O_3 nanoparticles, Zeng *et al.* produced Fe_2O_3/Au nanozyme with tandem enzymatic activity, including GOx-like activity.[144] The indigo-carmine method was employed to detect the presence of H_2O_2 produced from the oxidation of glucose. The tabulated result indicates that, similar to Au nanoparticles, Fe_2O_3/Au nanozyme exhibits GOx-like activity (6.4 U mL^{-1}). Additionally, the result of the cytometry test shown in Fig. 5e demonstrates the nanozyme's excellent ability to trigger cell death.

Fig. 5 (a) Fluorescence spectra of Fe-TCPP MOFs after the incubation with GSH.[139] Reproduced from ref. 139 with permission from American Chemical Society, Copyright 2024 (b) images of tumor at Fe_3S_4-injected mice (left) and photos of the dissected tumor from mice after the treatment.[140] Reproduced from ref. 140 with permission from Elsevier, Copyright 2023 (c) schematic on *in vivo* anti-tumor procedures; body weight, average tumor volumes, survival rate and tumor weights collected of different groups. G1: Control, G2; iRFA, G3: iRFA + TSN, G4: iRFA + Fe-SA/N-BCNT, G5: iRFA + TSN@Fe-SA/N-BCNT.[148] Reproduced from ref. 148 with permission from Wiley-VCH, Copyright 2024 (d) *in vivo* bioluminescence imaging of 4T1-Luc tumor-bearing mice on the fifth and twentieth days.[149] Reproduced from ref. 149 with permission from Elsevier, Copyright 2021 (e) the Annexin-FITC/PI apoptosis assay of Fe_2O_3/Au-PEG incubated with 4T1 cells.[144] Reproduced from ref. 144 with permission from Elsevier, Copyright 2023.

4.3. CAT-like activity

CAT is widely present in all aerobic organisms and some anaerobic organisms. It is a heme-containing enzyme that catalyzes the decomposition of less toxic H_2O_2 into O_2 and water (H_2O).[145] By mimicking this activity, nanomaterial-based enzymes have broad application prospects in improving tumor hypoxia, antibacterial therapy, cardiovascular diseases, and
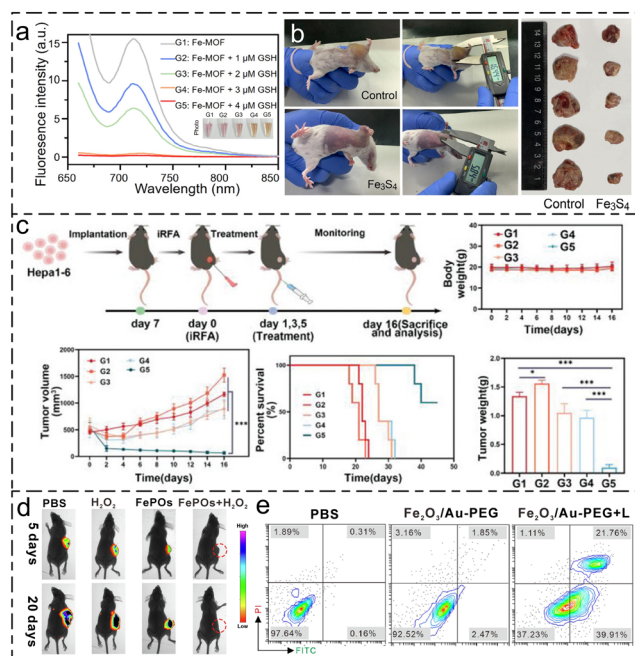
biosensing, among other fields.[146,147] Additionally, CAT-like activity constantly relieves the anaerobic environment within the tumor microenvironment to help enhance the cascade reaction efficiency.

Wang *et al.* synthesized a Fe-SA/N-BCNT SAzyme with mixed valence states of the Fe atom.[148] Its CAT-like activity was analyzed, revealing the results of the dissolved O_2 from the reaction of Fe-SA/N-BCNT in an excess H_2O_2 aqueous solution. While N-BCNT showed no O_2 evolution, the O_2 evolution index of Fe-SA/N-BCNT proved to be satisfactory; with an increase of nanozyme concentration, the amount of O_2 produced increased synchronously. As shown in Fig. 5c, the animal experiments on tumor suppression demonstrate the effective antitumor capability of the nanozyme, as characterized by tumor volume measurements. Additionally, the biosafety of the nanozyme was also evaluated.

4.4. SOD-like activity

SOD-like enzymes are important antioxidants that catalyze the decomposition of superoxide radicals ($\cdot O_2^-$) in the microenvironment into O_2 and the less toxic H_2O_2.[150] These enzymes effectively remove ROS, combat ageing, and mitigate inflammation.[151]

SOD-like activity is assessed by analysing the inhibition of pyrogallol autooxidation.[152] Under alkaline conditions, pyrogallol undergoes autoxidation, resulting in a product that shows an absorption peak at 412 nm under UV-Vis analysis. Wang *et al.* characterized the SOD-like enzymatic activity of iron-phosphate based FePOs nanozyme using this method.[149] The UV-Vis result conveys that in the absence of FePOs, the pyrogallol solution exhibits a strong absorption peak at wavelength 320 nm; however, this peak declines rapidly upon the addition of FePOs. The tumor inhibition ability of FePOs was evaluated using *in vivo* bioluminescence imaging of 4T1-Luc tumor-bearing mice on the 5th and 20th day of treatment. As shown in Fig. 5d, tumors in mice treated with H_2O_2 and FePOs disappeared after 20 days, while tumors in the other mice grew or remained constant.

5. Conclusion and prospectives

Iron-based nanozymes have emerged as a potent tool for tumor therapy through their ability to induce ferroptosis, a regulated form of cell death characterized by iron-mediated LPO. This review has examined various categories of iron-based nanozymes, including iron oxides, single-atom nanozymes, and iron-based MOFs, with each offering unique advantages in modulating ROS and disrupting cellular homeostasis in tumors. Their enzymatic activities—mimicking peroxidase, oxidase, catalase, and superoxide dismutase—enable precise control over ROS production within the tumor microenvironment (TME), thereby enhancing ferroptosis and reducing off-target toxicity to surrounding healthy cells. By integrating these catalytic properties with tumor-selective targeting mechanisms, iron-based nanozymes offer a promising approach to addressing therapeutic challenges like drug resistance and the need for targeted treatment. However, problems still exist in the clinical application regarding tumor treatment of iron-based nanozyme.

Notably, the biosafety of iron-based nanozymes requires further investigation, particularly for widely studied but high-risk nanozymes such as iron oxide nanoparticles. It has been proved that bare Fe_3O_4 nanoparticles possess low stability in a physiological environment and would generate harmful radicals *in vivo*.[54] While previous research has also demonstrated solutions for increasing the stability and biocapability by coating with certain materials, including polymer materials[153] and Au shell.[154] Furthermore, engineering pH-responsive coatings or enzyme-mimicking active sites (*e.g.*, $Fe-N_x$ centers) could enhance release specificity, enabling differentiation between pathological and healthy microenvironments. These chemical designs not only mitigate biosafety concerns but also relieve the translational potential risk of iron-based nanozymes.

Furthermore, the selectivity of enzymatic activity over redox substrates is a vital issue that should be combated for enhanced ferroptosis efficiency. As demonstrated in the previous passage, for POD-like activity and CAT-like activity, which both involve H_2O_2 as a reactant, the competitive reactions would limit the generation of ROS. Therefore, analyzing the competitive effect between these activities by modulating the structure of nanozymes, including the atomic distance of active sites and atomic defects on the nanozyme surface, is a possible future research direction of nanozyme development and design.

As a novel developed measure for clinical tumor therapy, nanozymes have been proven to exhibit tumor cell eliminating ability on mouse tumor models. However, current research prospects are based mainly on tumor cell lines, *e.g.* HeLa and 4T1, inoculated on mouse models, while the effect of triggering ferroptosis by nanozymes targeting specific tumor modelling, including lung cancer, colorectal cancer, hepatocellular carcinoma, gastric signet ring cell carcinoma, has unusually been reported. With the primary purpose of accelerating the clinical translation of nanozymes, the study based on specific tumor modelling of nanozymes should be applied in future nanozyme research.

In conclusion, further exploration based on novelly evolved analytical measures *e.g.* artificial intelligence (AI) and cryo-electronic microscopy (cryo-EM), is required to improve the catalytic mechanism of nanozymes. A thorough understanding of structure-activity relationship is essential to optimally design high-performance nanozymes. Although theoretical measures, including density functional theory (DFT) calculations and machine, learning have been applied to predict the catalytic activity of nanozymes, the cost of these measures is still high, and there are challenges surrounding differences in actual *versus* experimental catalytic activity results predicted by DFT. Therefore, the accumulation of results from further research would greatly enlarge the 'database' of nanozyme, thereby providing a promising theoretical basis for the application of nanozymes in tumor therapy.

Author contributions

C.D. and Z.Y. contributed equally to this work, regarding the writing, editing and finalization of the manuscript. J.G. conceived this work. C.J.Z., H.C. and J.G. revised the manuscript. All authors read and approved the final manuscript.

Data availability

No primary research results, software or code have been included, and no new data were generated or analyzed as part of this review.

Conflicts of interest

There are no conflicts of interest to declare.

Acknowledgements

References

1 F. Bray, M. Laversanne, H. Sung, J. Ferlay, R. L. Siegel, I. Soerjomataram and A. Jemal, *CA Cancer J. Clin.*, 2024, **74**, 229–263.

2 S. Tohme, R. L. Simmons and A. Tsung, *Cancer Res.*, 2017, **77**, 1548–1552.

3 R. Baskar, K. A. Lee, R. Yeo and K.-W. Yeoh, *Int. J. Med. Sci.*, 2012, **9**, 193.

4 K. Bukowski, M. Kciuk and R. Kontek, *Int. J. Mol. Sci.*, 2020, **21**, 3233.

5 L. Yang, Q. Ning and S.-S. Tang, *J. Immunol. Res.*, 2022, **2022**, 8052212.

6 Y. T. Lee, Y. J. Tan and C. E. Oon, *Eur. J. Pharmacol.*, 2018, **834**, 188–196.

7 B. R. Stockwell, J. P. F. Angeli, H. Bayir, A. I. Bush, M. Conrad, S. J. Dixon, S. Fulda, S. Gascón, S. K. Hatzios, V. E. Kagan, K. Noel, X. Jiang, A. Linkermann, M. E. Murphy, M. Overholtzer, A. Oyagi, G. C. Pagnussat, J. Park, Q. Ran, C. S. Rosenfeld, K. Salnikow, D. Tang, F. M. Torti, S. V. Torti, S. Toyokuni, K. A. Woerpel and D. D. Zhang, *Cell*, 2017, **171**, 273–285.

8 X. Chen, J. Li, R. Kang, D. J. Klionsky and D. Tang, *Autophagy*, 2021, **17**, 2054–2081.

9 D. Tang, R. Kang, T. V. Berghe, P. Vandenabeele and G. Kroemer, *Cell Res.*, 2019, **29**, 347–364.

10 C. Holohan, S. Van Schaeybroeck, D. B. Longley and P. G. Johnston, *Nat. Rev. Cancer*, 2013, **13**, 714–726.

11 N. Singh, D. Kim, S. Min, E. Kim, S. Kim, Y. S. Zhang, H. Kang and J. S. Kim, *Coord. Chem. Rev.*, 2025, **522**, 216236.

12 C. Liang, X. Zhang, M. Yang and X. Dong, *Adv. Mater.*, 2019, **31**, 1904197.

13 S. J. Dixon, K. M. Lemberg, M. R. Lamprecht, R. Skouta, E. M. Zaitsev, C. E. Gleason, D. N. Patel, A. J. Bauer, A. M. Cantley, W. S. Yang, B. Morrison III and B. R. Stockwell, *Cell*, 2012, **149**, 1060–1072.

14 I. Bano, P. Horky, S. Q. Abbas, M. Majid, A. H. M. Bilal, F. Ali, T. Behl, S. S. U. Hassan and S. Bungau, *Molecules*, 2022, **27**, 2129.

15 X. Chen, R. Kang, G. Kroemer and D. Tang, *Nat. Rev. Clin. Oncol.*, 2021, **18**, 280–296.

16 X. Jiang, B. R. Stockwell and M. Conrad, *Nat. Rev. Mol. Cell Biol.*, 2021, **22**, 266–282.

17 Y. Liu, R. Niu, R. Deng, S. Song, Y. Wang and H. Zhang, *J. Am. Chem. Soc.*, 2023, **145**, 8965–8978.

18 D. Wang, *Chem.-Biol. Interact.*, 2023, **371**, 110348.

19 Y. Wang, F. Chen, H. Zhou, L. Huang, J. Ye, X. Liu, W. Sheng, W. Gao, H. Yu and F. Wang, *Small Methods*, 2023, **7**, 2200888.

20 C. Wu, D. Xu, M. Ge, J. Luo, L. Chen, Z. Chen, Y. You, Y.-X. Zhu, H. Lin and J. Shi, *Nano Today*, 2022, **46**, 101574.

21 C. Wu, X. Han, W. Feng, Z. Liu, L. Chen, B. Zhou, Y. Chen and J. Shi, *Chem. Eng. J.*, 2021, **411**, 128543.

22 T. Liu, L. Sun, Y. Zhang, Y. Wang and J. Zheng, *J. Biochem. Mol. Toxicol.*, 2022, **36**, e22942.

23 B. Niu, K. Liao, Y. Zhou, T. Wen, G. Quan, X. Pan and C. Wu, *Biomaterials*, 2021, **277**, 121110.

24 L. Gao, J. Zhuang, L. Nie, J. Zhang, Y. Zhang, N. Gu, T. Wang, J. Feng, D. Yang, S. Perrett and X. Yan, *Nat. Nanotechnol.*, 2007, **2**, 577–583.

25 J.-Y. Lee, W. K. Kim, K.-H. Bae, S. C. Lee and E.-W. Lee, *Biology*, 2021, **10**, 184.

26 P. Dydio, H. Key, A. Nazarenko, J.-E. Rha, V. Seyedkazemi, D. Clark and J. Hartwig, *Science*, 2016, **354**, 102–106.

27 M. Liang and X. Yan, *Acc. Chem. Res.*, 2019, **52**, 2190–2200.

28 Y. Lin, J. Ren and X. Qu, *Acc. Chem. Res.*, 2014, **47**, 1097–1105.

29 J. Xie, X. Zhang, H. Wang, H. Zheng and Y. Huang, *TrAC, Trends Anal. Chem.*, 2012, **39**, 114–129.

30 M. Li, H. Zhang, Y. Hou, X. Wang, C. Xue, W. Li, K. Cai, Y. Zhao and Z. Luo, *Nanoscale Horiz.*, 2020, **5**, 202–217.

31 Y. Huang, J. Ren and X. Qu, *Chem. Rev.*, 2019, **119**, 4357–4412.

32 Q. Liu, A. Zhang, R. Wang, Q. Zhang and D. Cui, *Nano-Micro Lett.*, 2021, **13**, 1–53.

33 D. Wang, *Chem.-Biol. Interact.*, 2023, **371**, 110348.

34 Z. Dong, P. Liang, Y. Wang, G. Guan, L. Teng, R. Yue, C. Lu, S. Huan, X. Yin and G. Song, *J. Mater. Chem. B*, 2023, **11**, 5933–5952.

35 H. Zheng, S. Wang, S. Liu, J. Wu, J. Guan, Q. Li, Y. Wang, Y. Tao, S. Hu, Y. Bai, J. Wang, X. Xiong, Y. Xiong and Y. Lei, *Adv. Funct. Mater.*, 2023, **33**, 2300815.

36 Y. Du and Z. Guo, *Cell Death Discovery*, 2022, **8**, 501.

37 C. Wang, H. Xu, C. Liang, Y. Liu, Z. Li, G. Yang, L. Cheng, Y. Li and Z. Liu, *ACS Nano*, 2013, **7**, 6782–6795.

38 T.-H. Chung, J.-K. Hsiao, S.-C. Hsu, M. Yao, Y.-C. Chen, S.-W. Wang, M. Y.-P. Kuo, C.-S. Yang and D.-M. Huang, *ACS Nano*, 2011, **5**, 9807–9816.

39 X. Fang, D. Yang, X. Wu, K.-H. Lui, X. Li, W.-S. Lo, C. Li, Y. Zhang, G. Nie, L. Jiang, Y. Gu, B. Zhang and W.-T. Wang, *Chem. Eng. J.*, 2023, **474**, 145675.

40 M. Zhao, R. Yang, Y. Wei, J. Su, X. Wang, N. Zhang, P. Sun, D. Chen and Y. Zhao, *Nano Today*, 2022, **44**, 101493.

41 X. Wang, Q. Chen and C. Lu, *Molecules*, 2022, **27**, 4247.

42 X. Ma, X. Ren, X. Guo, C. Fu, Q. Wu, L. Tan, H. Li, W. Zhang, X. Chen, H. Zhong and X. Meng, *Biomaterials*, 2019, **214**, 119223.

43 P. Xue, H. Zhuang, T. Bai, X. Zeng, J. Deng, S. Shao and S. Yan, *J. Nanobiotechnol.*, 2024, **22**, 228.

44 P. Xue, H. Zhuang, S. Shao, T. Bai, X. Zeng and S. Yan, *ACS Nano*, 2024, **18**, 25795–25812.

45 X. Meng, D. Li, L. Chen, H. He, Q. Wang, C. Hong, J. He, X. Gao, Y. Yang, B. Jiang, G. Nie, X. Yan, L. Gao and K. Fan, *ACS Nano*, 2021, **15**, 5735–5751.

46 R. Kudarha, N. Dhas and S. Mutalik, *Coord. Chem. Rev.*, 2023, **494**, 215330.

47 M. J. Ko, S. Min, H. Hong, W. Yoo, J. Joo, Y. S. Zhang, H. Kang and D.-H. Kim, *Bioact. Mater.*, 2024, **32**, 66–97.

48 A. Mohapatra, A. Mohanty and I.-K. Park, *Cancers*, 2024, **16**, 3210.

49 H. Zheng, J. Jiang, S. Xu, W. Liu, Q. Xie, X. Cai, J. Zhang, S. Liu and R. Li, *Nanoscale*, 2021, **13**, 2266–2285.

50 Y. Ming, M. Huang, Y. Huang, D. Liu, M. Sun, B. Jia and J. Du, *Mater. Chem. Front.*, 2024, **8**, 1685–1709.

51 Y. Zhang, W. Yu, M. Chen, B. Zhang, L. Zhang and P. Li, *Nanoscale*, 2023, **15**, 12137–12156.

52 J. Han and J. Guan, *Coord. Chem. Rev.*, 2023, **490**, 215209.

53 L. Gao, K. Fan and X. Yan, *Theranostics*, 2017, **7**, 3207.

54 Q. Liu, A. Zhang, R. Wang, Q. Zhang and D. Cui, *Nano-Micro Lett.*, 2021, **13**, 154.

55 U. T. Bornscheuer, G. Huisman, R. Kazlauskas, S. Lutz, J. Moore and K. Robins, *Nature*, 2012, **485**, 185–194.

56 A. F. Gualtieri, G. B. Andreozzi, M. Tomatis and F. Turci, *Free Radicals Biol. Med.*, 2019, **133**, 21–37.

57 D. Stoyanovsky, Y. Tyurina, I. Shrivastava, I. Bahar, V. Tyurin, O. Protchenko, S. Jadhav, S. Bolevich, A. Kozlov, Y. Vladimirov, A. Shvedova, C. Philpott, H. Bayir and V. Kagan, *Free Radicals Biol. Med.*, 2019, **133**, 153–161.

58 Y. Yin, R. Lv, W. Zhang, J. Lu, Y. Ren, X. Li, L. Lv, M. Hua and B. Pan, *Appl. Catal., B*, 2021, **295**, 120282.

59 Y. Yin, Y. Zhang, B. Wu, L. Hu, Y. Wang, J. Wan and W. Zhang, *Appl. Catal., B*, 2024, **340**, 123165.

60 H. Dong, W. Du, J. Dong, R. Che, F. Kong, W. Cheng, M. Ma, N. Gu and Y. Zhang, *Nat. Commun.*, 2022, **13**, 5365.

61 S. Li, H. Ding, J. Chang, S. Dong, B. Shao, Y. Dong, S. Gai, F. He and P. Yang, *J. Colloid Interface Sci.*, 2022, **623**, 787–798.

62 S. Y. Yin, G. Song, Y. Yang, Y. Zhao, P. Wang, L. M. Zhu, X. Yin and X. B. Zhang, *Adv. Funct. Mater.*, 2019, **29**, 1901417.

63 F. Gong, N. Yang, Y. Wang, M. Zhuo, Q. Zhao, S. Wang, Y. Li, Z. Liu, Q. Chen and L. Cheng, *Small*, 2020, **16**, 2003496.

64 G. Tang, J. He, J. Liu, X. Yan and K. Fan, Nanozyme for tumor therapy: Surface modification matters, Wiley Online Library, 2021, vol. 1, pp. 75–89.

65 Y. Chen, W. Xu, H. Jin, M. Zhang, S. Liu, Y. Liu and H. Zhang, *ACS Nano*, 2024, **18**, 31846–31868.

66 C. Peng, R. Pang, J. Li and E. Wang, *Adv. Mater.*, 2024, **36**, 2211724.

67 S. Ji, B. Jiang, H. Hao, Y. Chen, J. Dong, Y. Mao, Z. Zhang, R. Gao, W. Chen, R. Zhang, Q. Liang, H. Li, S. Liu, Y. Wang, Q. Zhang, L. Gu, D. Duan, M. Liang, D. Wang, X. Yan and Y. Li, *Nat. Catal.*, 2021, **4**, 407–417.

68 S. Zhang, X. J. Gao, Y. Ma, K. Song, M. Ge, S. Ma, L. Zhang, Y. Yuan, W. Jiang, Z. Wu, L. Gao, X. Yan and B. Jiang, *Nat. Commun.*, 2024, **15**, 10605.

69 D. Choi, H. Jung, J. Im, S. Y. Yi, S. Kim, D. Lee, S. Park, C. Lee, J. Kim, J. W. Han and J. Lee, *Adv. Mater.*, 2024, **36**, 2306602.

70 R. Xu, R. Sun, H.-Q. Xu, G. Xie and J. Ge, *J. Mater. Chem. A*, 2024, **12**, 26316–26349.

71 R. Zeng, Q. Gao, L. Xiao, W. Wang, Y. Gu, H. Huang, Y. Tan, D. Tang and S. Guo, *J. Am. Chem. Soc.*, 2024, **146**, 10023–10031.

72 H. Zhang, P. Wang, J. Zhang, Q. Sun, Q. He, X. He, H. Chen and H. Ji, *Angew. Chem., Int. Ed.*, 2024, **63**, e202316779.

73 Z. Lin, D. Liao, C. Jiang, A. Nezamzadeh-Ejhieh, M. Zheng, H. Yuan, J. Liu, H. Song and C. Lu, *RSC Med. Chem.*, 2023, **14**, 1914–1933.

74 Y. Yuan, B. Chen, X. An, Z. Guo, X. Liu, H. Lu, F. Hu, Z. Chen, C. Guo and C. M. Li, *Adv. Healthcare Mater.*, 2024, **13**, 2304591.

75 Q. Wang and D. Astruc, *Chem. Rev.*, 2020, **120**, 1438–1511.

76 C. Shuai, J. Zan, F. Deng, Y. Yang, S. Peng and Z. Zhao, *ACS Sustainable Chem. Eng.*, 2021, **9**, 1814–1825.

77 Z. Chen, Y. Sun, J. Wang, X. Zhou, X. Kong, J. Meng and X. Zhang, *ACS Nano*, 2023, **17**, 9003–9013.

78 Z. Liu, S. Liu, B. Liu, Q. Meng, M. Yuan, X. Ma, J. Wang, P. A. Ma and J. Lin, *Adv. Funct. Mater.*, 2024, **34**, 2407153.

79 C. Fang, Z. Deng, G. Cao, Q. Chu, Y. Wu, X. Li, X. Peng and G. Han, *Adv. Funct. Mater.*, 2020, **30**, 1910085.

80 J. Lu, Y. Yang, Q. Xu, Y. Lin, S. Feng, Y. Mao, D. Wang, S. Wang and Q. Zhao, *Coord. Chem. Rev.*, 2023, **474**, 214861.

81 F. Yang, J. Dong, Z. Li and Z. Wang, *ACS Nano*, 2023, **17**, 4102–4133.

82 T. Wang, C. Wang, Y. Wang, X. Zhang, X. Cai, Z. Guo, X. Meng, X. Jiang, Y. Wu, Y. Cao, C. Zuo and W. Bu, *Adv. Funct. Mater.*, 2024, **34**, 2400791.

83 J. You, S. Liu, J. Liang, Q. Feng, M. Duan, Z. Ali, L. Chen and Z. Wang, *Med. Mat.*, 2024, **1**, 104–117.

84 L.-G. Li, X.-X. Yang, H.-Z. Xu, T.-T. Yu, Q.-R. Li, J. Hu, X.-C. Peng, N. Han, X. Xu, N.-N. Chen, X. Chen, J.-M. Tang and T.-F. Li, *Adv. Healthcare Mater.*, 2023, **12**, 2301561.

85 L. Sutrisno, Y. Hu, Y. Hou, K. Cai, M. Li and Z. Luo, *Front. Chem.*, 2020, **8**, 680.

86 M. Xu, F. Lai, H. Liu, D. Hu, Y. Sun, F. Li, M. Sun, N. Lv, B. Qiu, Y. Pan and Y. Hu, *Chem. Eng. J.*, 2024, **500**, 156920.

87 C. Cao, Y. Lu, X. Pan, Y. Lin, S. Fan, J. Niu, S. Lin, H. Tan, Y. Wang, S. Cui and Y. Liu, *Adv. Healthcare Mater.*, 2024, **13**, 2304249.

88 C. Yao, R. Zhang, Z. Xie, Y. Wu and X. Wu, *Small*, 2025, 2409026.

89 M. Li, H. Zhang, Y. Hou, X. Wang, C. Xue, W. Li, K. Cai, Y. Zhao and Z. Luo, *Nanoscale Horiz.*, 2020, **5**, 202–217.

90 S. J. Dixon and B. R. Stockwell, *Annu. Rev. Cancer Biol.*, 2019, **3**, 35–54.

91 R. Kang, G. Kroemer and D. Tang, *Free Radicals Biol. Med.*, 2019, **133**, 162–168.

92 A. Hafner, M. L. Bulyk, A. Jambhekar and G. Lahav, *Nat. Rev. Mol. Cell Biol.*, 2019, **20**, 199–210.

93 B. Chu, N. Kon, D. Chen, T. Li, T. Liu, L. Jiang, S. Song, O. Tavana and W. Gu, *Nat. Cell Biol.*, 2019, **21**, 579–591.

94 C. Liang, X. Zhang, M. Yang and X. Dong, *Adv. Mater.*, 2019, **31**, 1904197.

95 W. S. Yang and B. R. Stockwell, *Chem. Biol.*, 2008, **15**, 234–245.

96 M. M. Gaschler and B. R. Stockwell, *Biochem. Biophys. Res. Commun.*, 2017, **482**, 419–425.

97 H. Feng and B. R. Stockwell, *PLoS Biol.*, 2018, **16**, e2006203.

98 R. Shah, K. Margison and D. A. Pratt, *ACS Chem. Biol.*, 2017, **12**, 2538–2545.

99 W. Wang, M. Green, J. E. Choi, M. Gijón, P. D. Kennedy, J. K. Johnson, P. Liao, X. Lang, I. Kryczek and A. Sell, *Nature*, 2019, **569**, 270–274.

100 A. R. Bogdan, M. Miyazawa, K. Hashimoto and Y. Tsuji, *Trends Biochem. Sci.*, 2016, **41**, 274–286.

101 I. Bano, P. Horky, S. Q. Abbas, M. Majid, A. H. M. Bilal, F. Ali, T. Behl, S. S. U. Hassan and S. Bungau, *Molecules*, 2022, **27**, 2129.

102 C. Cao, X. Wang, N. Yang, X. Song and X. Dong, *Chem. Sci.*, 2022, **13**, 863–889.

103 Z. Yi, X. Yang, Y. Liang, F. Chapelin and S. Tong, *Small*, 2024, **20**, 2305974.

104 C. Zhang, S. Lu, K. Deng, W. Qian, Y. Liu, Y. Li, S. Jin, R. Suo, H. Xu and B. Wu, *Adv. Funct. Mater.*, 2023, **33**, 2301462.

105 Z. Jie, B. Xiong and J. Shi, *Adv. Sci.*, 2024, **11**, 2402801.

106 L. Zhang, W. Wang, M. Ou, X. Huang, Y. Ma, J. Tang, T. Hou, S. Zhang, L. Yin, H. Chen, Y. Hou and Y. Ding, *Nano Res.*, 2022, **15**, 4310–4319.

107 W. S. Yang, R. SriRamaratnam, M. E. Welsch, K. Shimada, R. Skouta, V. S. Viswanathan, J. H. Cheah, P. A. Clemons, A. F. Shamji, C. B. Clish, L. M. Brown, A. W. Girotti, V. W. Cornish, S. L. Schreiber and B. R. Stockwell, *Cell*, 2014, **156**, 317–331.

108 M. Aldrovandi, M. Fedorova and M. Conrad, *Trends Endocrinol. Metab.*, 2021, **32**, 463–473.

109 F. Ursini and M. Maiorino, *Free Radicals Biol. Med.*, 2020, **152**, 175–185.

110 E. Niki, *Free Radicals Biol. Med.*, 2009, **47**, 469–484.

111 J. Sun, J. S. Fleishman, X. Liu, H. Wang and L. Huo, *Biomed. Pharmacother.*, 2024, **174**, 116453.

112 Y. Zhu, X. Niu, T. Wu, J. Cheng, J. Zou, Y. Pan, Y. Tian, W. Huang, C. Ding, Y. Lin, D. Kang and X. Chen, *Chem. Eng. J.*, 2024, **485**, 150126.

113 B. Li, R. Ma, L. Chen, C. Zhou, Y.-X. Zhang, X. Wang, H. Huang, Q. Hu, X. Zheng, J. Yang, M. Shao, P. Hao, Y. Wu, Y. Che, C. Li, T. Qin, L. Gao, Z. Niu and Y. Li, *Nat. Commun.*, 2023, **14**, 7312.

114 X. Xiao, M. Chen, Y. Zhang, L. Li, Y. Peng, J. Li and W. Zhou, *J. Nanobiotechnol.*, 2022, **20**, 410.

115 R. Yazdian-Robati, P. Bayat, F. Oroojalian, M. Zargari, M. Ramezani, S. M. Taghdisi and K. Abnous, *Int. J. Biol. Macromol.*, 2020, **155**, 1420–1431.

116 Y. Liu, R. Niu, R. Deng, S. Song, Y. Wang and H. Zhang, *J. Am. Chem. Soc.*, 2023, **145**, 8965–8978.

117 W. Liu, Q. Chen, J. Wu, F. Zhang, L. Han, J. Liu, H. Zhang, Z. Hao, E. Shi, Y. Sun, R. Zhang, Y. Wang and L. Zhang, *Adv. Funct. Mater.*, 2024, **34**, 2312308.

118 P. Kuppusamy, H. Li, G. Ilangovan, A. J. Cardounel, J. L. Zweier, K. Yamada, M. C. Krishna and J. B. Mitchell, *Cancer Res.*, 2002, **62**, 307–312.

119 Y. Ming, M. Huang, Y. Huang, D. Liu, M. Sun, B. Jia and J. Du, *Mater. Chem. Front.*, 2024, **8**, 1685–1702.

120 S. Wang, R. Ma, Z. Mei and Y. Hou, *Med. Mat.*, 2024, **1**, 6–26.

121 F. Wu, Y. Du, J. Yang, B. Shao, Z. Mi, Y. Yao, Y. Cui, F. He, Y. Zhang and P. Yang, *ACS Nano*, 2022, **16**, 3647–3663.

122 B. C. Dickinson and C. J. Chang, *Nat. Chem. Biol.*, 2011, **7**, 504–511.

123 G. J. Kim, K. Chandrasekaran and W. F. Morgan, *Mutagenesis*, 2006, **21**, 361–367.

124 M. Khanmohammadi, M. B. Dastjerdi, A. Ai, A. Ahmadi, A. Godarzi, A. Rahimi and J. Ai, *Biomater. Sci.*, 2018, **6**, 1286–1298.

125 K. Wan, B. Jiang, T. Tan, H. Wang and M. Liang, *Small*, 2022, **18**, 2204372.

126 Y. Han, K. Ge, Y. Zhao, M. Bottini, D. Fan, W. Wu, L. Li, F. Liu, S. Gao, X. J. Liang and J. Zhang, *Small*, 2024, **20**, 2306656.

127 L. Jiao, W. Xu, Y. Zhang, Y. Wu, W. Gu, X. Ge, B. Chen, C. Zhu and S. Guo, *Nano Today*, 2020, **35**, 100971.

128 C. Yao, R. Zhang, Z. Xie, Y. Wu and X. Wu, *Small*, 2025, **21**, 2409026.

129 D. Wang, H. Wu, C. Wang, L. Gu, H. Chen, D. Jana, L. Feng, J. Liu, X. Wang, P. Xu, Z. Guo, Q. Chen and Y. Zhao, *Angew. Chem.*, 2021, **133**, 3038–3044.

130 I. O. L. Bacellar, T. M. Tsubone, C. Pavani and M. S. Baptista, *Int. J. Mol. Sci.*, 2015, **16**, 20523–20559.

131 D. Li, Y. Tong, J. Huang, L. Ding, Y. Zhong, D. Zeng and P. Yan, *J. Mol. Catal. A: Chem.*, 2011, **345**, 108–116.

132 Y. Qin, Q. Wang, M. Qian and R. Huang, *Mater. Today*, 2024, **76**, 28–39.

133 D. Van Straten, V. Mashayekhi, H. S. De Bruijn, S. Oliveira and D. J. Robinson, *Cancers*, 2017, **9**, 19.

134 Y.-Q. He and J.-H. Tang, *Adv. Healthcare Mater.*, 2025, **14**, 2403009.

135 Y. Feng, Y. Shi, Q. Zhao, G. Gao, Z. Wang and J. Zhi, *J. Colloid Interface Sci.*, 2025, **681**, 205–214.

136 H. Liu, B. Yu, P. Yang, Y. Yang, Z. Deng, X. Zhang, K. Wang and H. Wang, *Adv. Sci.*, 2024, **11**, 2307254.

137 S. C. Lu, *Mol. Aspects Med.*, 2009, **30**, 42–59.

138 L. Kelland, *Nat. Rev. Cancer*, 2007, **7**, 573–584.

139 Z. Fan, S. Wu, H. Deng, G. Li, L. Huang and H. Liu, *ACS Nano*, 2024, **18**, 12261–12275.

140 A. Wu, M. Han, H. Ding, H. Rao, Z. Lu, M. Sun, Y. Wang, Y. Chen, Y. Zhang, X. Wang and D. Chen, *Chem. Eng. J.*, 2023, **474**, 145920.

141 S. Dong, W. Li, X. Li, Z. Wang, Z. Chen, H. Shi, R. He, C. Chen and W. Zhou, *Front. Immunol.*, 2022, **13**, 1038650.

142 Z. Ye, Y. Wang, G. Zhang, X. Hu, J. Wang and X. Chen, *J. Colloid Interface Sci.*, 2025, **678**, 380–392.

143 J. Ming, T. Zhu, W. Yang, Y. Shi, D. Huang, J. Li, S. Xiang, J. Wang, X. Chen and N. Zheng, *ACS Appl. Mater. Interfaces*, 2020, **12**, 51249–51262.

144 X. Zeng, Y. Ruan, Q. Chen, S. Yan and W. Huang, *Chem. Eng. J.*, 2023, **452**, 138422.

145 C. H. Tonial, M. F. Rodrigues, M. A. Bosse, I. M. Sousa, J. D. de Lima, M. A. A. da Cunha, M. A. Foglio, M. O. M. Marques and J. A. Marchese, *Ind. Crops Prod.*, 2020, **154**, 112650.

146 F. Wang, E. Ju, Y. Guan, J. Ren and X. Qu, *Small*, 2017, **13**, 1603051.

147 C. Xu and X. Qu, *NPG Asia Mater.*, 2014, **6**, e90.

148 Q. Wang, X. Zhu, B. Yin, K. Yan, G. Qiu, X. Liang, R. Jia, J. Chen, X. Wang, Y. Wu, J. Liu, J. Zhong, K. Zhang and D. Wang, *Adv. Funct. Mater.*, 2024, **34**, 2408141.

149 Z. Wang, G. Li, Y. Gao, Y. Yu, P. Yang, B. Li, X. Wang, J. Liu, K. Chen, J. Liu and W. Wang, *Chem. Eng. J.*, 2021, **404**, 125574.

150 Q. Fu, C. Wei and M. Wang, *ACS Nano*, 2024, **18**, 12049–12095.

151 X. Zhang, X. Chen and Y. Zhao, *Nano-Micro Lett.*, 2022, **14**, 95.

152 S. Marklund and G. Marklund, *Eur. J. Biochem.*, 1974, **47**, 469–474.

153 Z. Ye, Y. Fan, T. Zhu, D. Cao, X. Hu, S. Xiang, J. Li, Z. Guo, X. Chen, K. Tan and Z. Nanfeng, *ACS Appl. Mater. Interfaces*, 2022, **14**, 23194–23205.

154 S. V. Salihov, Y. A. Ivanenkov, S. P. Krechetov, M. S. Veselov, N. V. Sviridenkova, A. G. Savchenko, N. L. Klyachko, Y. I. Golovin, N. V. Chufarova, E. K. Beloglazkina and A. G. Majouga, *J. Magn. Magn. Mater.*, 2015, **394**, 173–178.